Density measurements using coherence imaging spectroscopy based on Stark broadening[a)]

O. Lischtschenko,[1,b)] K. Bystrov,[1] G. De Temmerman,[1] J. Howard,[2] R. J. E. Jaspers,[3] and R. König[4]
[1]*Association EURATOM-FOM, FOM-Institute for Plasma Physics Rijnhuizen, partner in the Trilateral Euregio Cluster, P.O. Box 1207, 3430 BE Nieuwegein, The Netherlands*
[2]*Research Laboratory, Australian National University, Canberra, Australian Capital Territory 0200, Australia*
[3]*Fusion Group, Eindhoven University of Technology, Postbus 513, 5600 MB Eindhoven, The Netherlands*
[4]*EURATOM Association, Max-Planck-Institut für Plasmaphysik, TI Greifswald, Wendelsteinstr.1, D-17491 Greifswald, Germany*

(Presented 20 May 2010; received 14 May 2010; accepted 2 August 2010; published online 19 October 2010)

A coherence imaging camera has been set up at Pilot-PSI. The system is to be used for imaging the plasma density through the Stark effect broadening of the H_γ line. Local density values are then obtained by the Abel inversion of the measured interferometric fringe contrast. This report will present the instrument setup and proof-of-principle demonstration. The inverted spatial electron density profiles obtained near the cascaded arc source of Pilot-PSI in discharges with axial magnetic field of $B=0.4$ T are compared with an independent measurement of electron density by Thomson scattering and good agreement is found. © *2010 American Institute of Physics.*
[doi:10.1063/1.3490023]

I. INTRODUCTION

Offering the Jacquinot (throughput) advantage and the ability of obtaining 2D spectral information Fourier transform spectrometers (imaging interferometers) have some potential advantages over slit-coupled grating spectrometers.[1] In the past few years the development of such coherence imaging systems using a variety of techniques has found applications in plasma Doppler and polarization spectroscopy.[2] The key to the application of coherence imaging techniques is the option for successfully describing the content of a spectral feature by a sufficiently small number of free parameters. For example, for the Doppler broadening of a spectral line, there are three free parameters—the brightness, and the spectral width and shift. These parameters can be recovered from measurements of the complex coherence (phase and amplitude of the interferogram) around an appropriately chosen optical delay.

In this paper, we report on the installation of a coherence imaging spectrometer (CIS) at the linear plasma generator Pilot-PSI.[3] In the configuration presented here, we measure the interferometric fringe contrast associated with the Stark broadening of the Balmer-γ line. We show that the contrast projection can be Abel inverted to obtain the electron density profile.

II. PILOT-PSI EXPERIMENTAL SETUP

All of the presented measurements have been conducted at Pilot-PSI, situated at the FOM Institute for Plasma Physics "Rijnhuizen". Pilot-PSI is a forerunner experiment to the larger facility Magnum-PSI (Ref. 3) nearing completion. Pilot- and Magnum-PSI are linear plasma generators capable of providing ITER-and-beyond plasma fluxes to target samples for plasma-wall interaction studies.[4] Pilot-PSI consists of a 1 m long and 40 cm diameter stainless steel vacuum vessel placed inside five coils producing an axial magnetic field of up to $B_z=1.6$ T. It is schematically displayed in Fig. 1.

The plasma source is a cascaded arc,[5] exhausting into the vessel along the magnetic field axis (z-direction). The source is usually operated in hydrogen with a typical gas flow of 2.0 slm$=8.8\times10^{20}$ H_2/s and discharge current of 100–200 A. The target is at 0.56 m distance from the nozzle of the source. Thomson scattering (TS) is employed at either 38 mm distance to the source nozzle or 17 mm in front of the target for determining the source or exposure conditions. TS results near the source confirmed a large experimental window spanning electron densities from 5×10^{19} to 4×10^{21} m^{-3} and electron temperatures between 0.1 and 4 eV.[6] At standard conditions of 150 A, 2.0 SLM H_2, and $B_z=0.4$ T, the center electron density as measured with the Thomson scattering is $\sim2\times10^{20}$ m^{-3}.

III. COHERENCE IMAGING SPECTROMETER

A "coherence imaging" spectrometer (CIS) is essentially an imaging polarization interferometer. The conceptual layout of a time-multiplex CIS system is shown at the bottom

[a)]Contributed paper, published as part of the Proceedings of the 18th Topical Conference on High-Temperature Plasma Diagnostics, Wildwood, New Jersey, May 2010.
[b)]Author to whom correspondence should be addressed. Electronic mail: lischtschenko@rijnhuizen.nl.

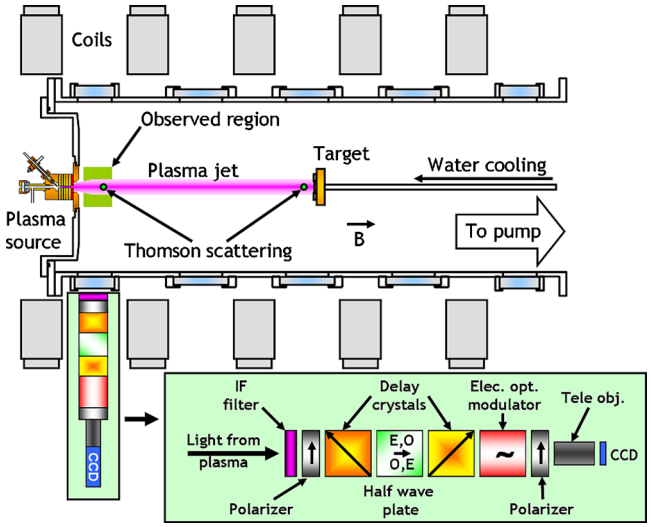

FIG. 1. (Color online) Schematic layout of Pilot-PSI and CIS setup at the right hand side (RHS) source observation port and observed region.

part of Fig. 1. The spectral range of interest is first isolated by means of a narrow band interference filter. Here a 1 nm full width at half maximum (FWHM) wide interference filter around 434.1 nm selects the wavelength area around H_γ, rejecting the rest of the spectrum. The transmitted light is imaged through a field-widened birefringent delay plate sandwiched between two polarizers onto a charge coupled device (CCD) camera to produce an image of the interferogram at a temporal offset fixed by the delay plate thickness. The delay is chosen to be comparable with the expected optical coherence length of the viewed spectrum. An electro-optically modulated birefringent plate is used to step-scan the optical path difference synchronously with the camera frame rate in order to allow images of the fringe contrast and phase to be recovered. A detailed description of the system can be found in Ref. 7. The employed camera is a Sensicam qe with 1376×1040 pixel resolution. The Sensicam is equipped with a Nikon Nikkor 28–105 mm f/3.5–4.5 zoom lens. The spatial resolution of the presented measurements is 82×82 μm^2/pixel (2×2 binning). The maximum temporal resolution of the current system is set by the maximum camera frame rate of 24 frames/s.

For quasimonochromatic radiation, the signal obtained at the image plane of the camera can be written as[7,8]

$$S(t) = 0.5I_0[1 + \zeta \cos(\varphi_m + \varphi_0)], \tag{1}$$

with fringe contrast ζ related to the optical coherence length at phase offset $\varphi_0 = 2\pi LB/\lambda_0$, where L is the delay plate thickness, B is its birefringence, and λ_0 is the "mean" wavelength. In order to recover the local fringe amplitude and phase, the phase steps ϕ_m introduced by the modulator are usually set at 0, $\pi/2$, and π, as described in Refs. 7 and 8. Usually, cameras with narrow band filters are employed to image plasma emission in 2D. That information is contained in CIS data as zero order moment. For the case of H_γ emission the situation with magnetic field is as displayed in Fig. 2.

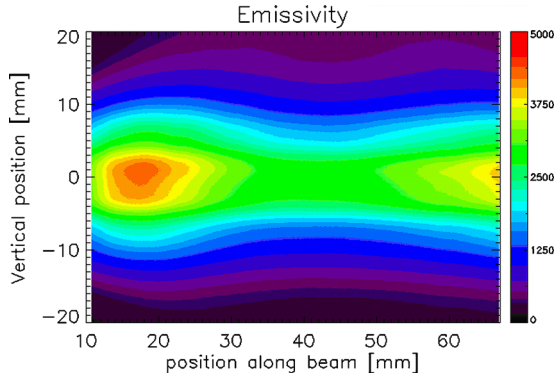

FIG. 2. (Color online) H_γ emission near the source of Pilot-PSI in operation with 2 SLM H_2 and magnetic field B=0.4 T.

IV. COHERENCE IMAGING OF HYDROGEN H_γ STARK-BROADENED EMISSION

When the plasma is inhomogeneous, the fringe quantities are line-integrated quantities, and in order to obtain local data, inversion of the line-of-sight integration is required. For example, the brightness is simply the line-integrated local emissivity

$$I_0 = \int e(r)dl. \tag{2}$$

For the case of H_γ the extracted brightness image I_0 with magnetic field energized is shown in Fig. 2. The image has been corrected for vignetting by applying a flat field calibration image obtained using a tungsten lamp and integrating sphere.

The image shows that the beam stays well collimated when the field is on and exhibits reasonable radial symmetry. While the brightness can be Abel inverted, interpretation is difficult as the emissivity is typically a function of many parameters, such as density and temperature.

In the case of the Doppler broadened line emission from inhomogeneous plasmas, the fringe contrast and phase deliver well-defined line integrals of quantities related directly to plasma temperature and flow.[8] For Stark broadening the Lorentzian line-shape can be characterized solely in terms of its spectral width. Given that the optical coherence is related to the Fourier transform of the spectral line-shape, it is straightforward to show that the fringe contrast in this case is proportional to

$$I_0\zeta = \int e(r)\exp(-\Gamma\hat{\varphi}_0/2)dl, \tag{3}$$

where $e(r)$ is the emissivity at position r in the plasma, $\Gamma(r)$ is the local spectral full width at half maximum normalized to the center wavelength and where the quantity $\hat{\varphi}_0$ is the group phase delay (proportional to φ_0).[3]

It is known from previous research on Pilot-PSI (Ref. 10) that Stark broadening is the dominant line broadening mechanism when looking at the emission of the H($n=5->2$) transition at 434.0466 nm. According to Griem's

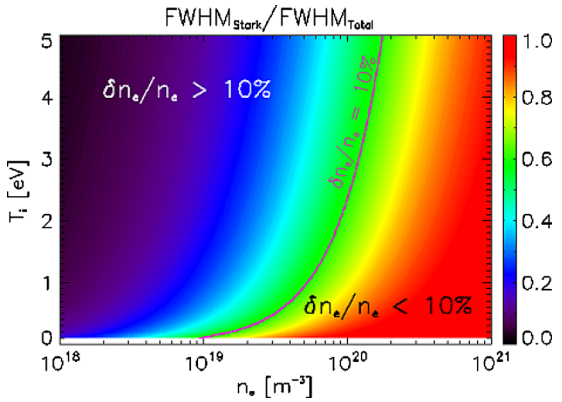

FIG. 3. (Color online) Ratio of the Stark broadening to total line broadening of the H_γ line for the Pilot-PSI parameter range; line indicates a 10% systematic relative density error due to approximating the line-shape with a single Lorentzian instead of a Voigt profile.

formula[9] the following scaling has been found:

$$\Gamma_{\mathrm{FWHM}}(\mathrm{nm}) = 0.0497 n_e^{2/3} (10^{20}\ \mathrm{m}^{-3}). \tag{4}$$

According to Ref. 10 this scaling is well fulfilled for electron densities n_e above 10^{20} m^{-3} and ion temperatures around 1 eV. Due to experimental limitations verification of the scaling above 10^{21} m^{-3} has not yet been tested. As can be seen from Fig. 3 Doppler broadening is usually less than half of the total broadening of the line. In the remainder of this work we ignore the Doppler contribution.

Equations (2) and (3) can be combined to obtain an expression for the local fringe contrast function

$$\zeta(r) = \exp\left[-\left(\frac{n_e}{n_c}\right)^{2/3}\right], \tag{5}$$

where n_c is a "characteristic" density set by the chosen optical path delay. Ignoring line integration effects, Eq. (3) can be used to calculate the contrast as function of optical path difference as shown in Fig. 4. A $LiNbO_3$ birefringent delay plate with thickness of 15 mm (obtained by combining two crystals of 7.5 mm each in a field-widened arrangement) is found to give a good dynamic range over the expected density regime ranging from $\sim 10^{19}$ up to 5×10^{20} m^{-3}.

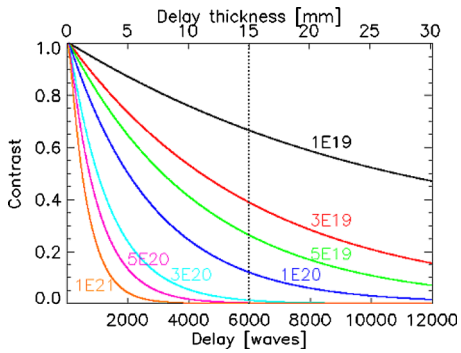

FIG. 4. (Color online) Fringe contrast as function of wave delay for various electron densities (dotted line indicates chosen delay).

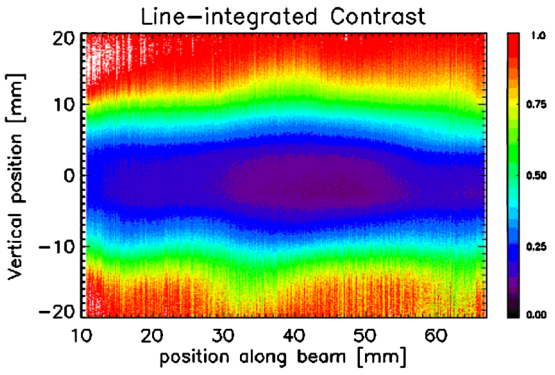

FIG. 5. (Color online) Line-integrated contrast map of the same Pilot-PSI discharge.

V. COHERENCE IMAGING OF HYDROGEN H_γ STARK-BROADENED EMISSION

The coherence imaging system is typically located at the first window on the RHS of Pilot-PSI (see Fig. 1). The measured contrast image associated with Fig. 2 is shown in Fig. 5. Note that the contrast decreases toward the plasma center, indicating a broadening of the spectral line (decrease in optical coherence) associated with higher electron densities. The image also shows reasonable radial symmetry and so is amenable to Abel inversion. The contrast has been corrected for the instrument contrast function (equivalent to the slit-function in a grating spectrometer) obtained by recording the instrument response to illumination by a hydrogen low pressure discharge lamp.

A. Inversion

For the Gaussian-shaped emission intensity profiles observed in Pilot-PSI, the inversion of the emission intensity can be directly calculated using the inertia of the Gaussian function to line-of-sight integration.[11] As this profile shows a dip in the central region a hollow profile is expected. Alternatively, the profile can be inverted using singular value decomposition (SVD) applied to the appropriately discretized version of Eq. (2) under the assumption of cylindrical symmetry. A comparison of the results is given in Fig. 6 showing that the Gaussian approach overestimates the center value while underestimating the wings of the profile.

The SVD method is hence used in further analysis as it does not make such strong assumptions. Applying this pro-

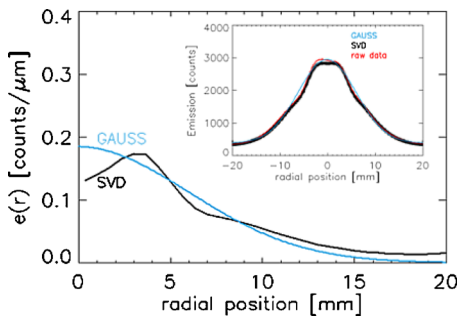

FIG. 6. (Color online) Inversion of the emission intensity at the TS position (38 mm from nozzle) with different models. Inset: line-integrated emission intensity of the two models and flat field corrected raw data.

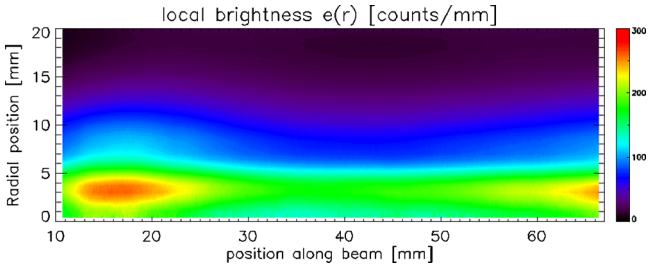

FIG. 7. (Color online) Local brightness obtained from SVD inversion of the measured emission intensity.

cedure to the whole image gives a local brightness image (using the SVD method), as shown in Fig. 7. Observe that following the beam expansion zone the emission intensity is reduced over a region of about 20 mm before it begins to rise again.

The inversion of Eq. (3) yields the local intensity weighted contrast $e(r)\zeta(r)$. After dividing by the local brightness obtained as above, the local contrast can be related to the density using Eq. (5), with $n_c = 3.15 \times 10^{19}$ m^{-3} being the characteristic density for the selected 15 mm delay plate thickness. The reconstructed density profile can be compared to the profile obtained from the Thomson scattering at the TS position near the source (see Fig. 8).

As can be seen the results match well except for the region between 2 and 7 mm. This is because the measured contrast almost vanishes in this region, and is smaller than the estimated uncertainty in the fringe contrast measurement, as shown in Fig. 9. This problem can be overcome by using a crystal plate of smaller delay (lower n_c).

VI. CONCLUSIONS AND OUTLOOK

A coherence imaging spectrometer has been installed on Pilot-PSI. Using the Stark broadening of the H_γ emission and inversion algorithms the coherence imaging system yields 2D local brightness and electron density maps. The measurement principle has been checked with the Thomson scattering. Good agreement has been found. Although local values can only be obtained by inversion, the inherent 2D measurement capability of the CIS, as well as its rather simple setup, can have practical advantages over TS in practical application. In more detail this means freeing three to six ports for other diagnostics in comparison to Thomson scattering. The quantitative analysis of the obtained local brightness images allows further exploitation in combination with collisional radiative models for simultaneous determination of the localized electron temperature.

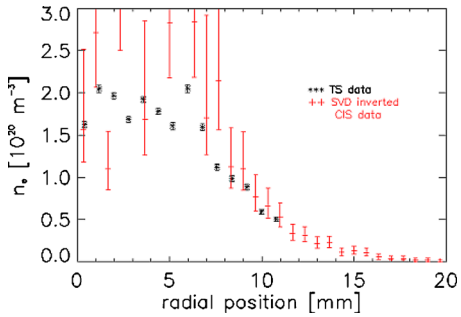

FIG. 8. (Color online) Comparison of the Abel inverted density obtained by CIS (at TS position) and direct measurement from the Thomson scattering (CIS data SVD inverted with 31 shells+bg).

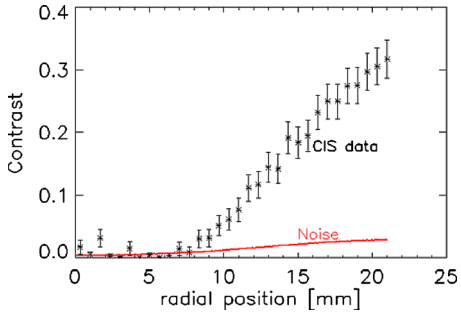

FIG. 9. (Color online) Local contrast obtained from SVD and corresponding noise contrast; error bars represent statistical errors.

ACKNOWLEDGMENTS

This work, supported by the European Communities under the contract of the Association EURATOM/FOM, was carried out within the framework of the European Fusion Programme with financial support from NWO. The views and opinions expressed herein do not necessarily reflect those of the European Commission. This work was carried out under the joint research project of "Coherence Imaging Spectroscopy on divertor-like plasmas" established between the Max-Planck-Institut für Plasmaphysik (IPP) and the Foundation for Fundamental Research on Matter (FOM).

[1] P. Jacquinot, J. Opt. Soc. Am. **44**, 761 (1954).
[2] J. Howard, C. Michael, F. Glass, and A. D. Cheetham, Rev. Sci. Instrum. **72**, 888 (2001).
[3] J. Rapp, W. R. Koppers, H. J. N. van Eck, G. J. van Rooij, W. J. Goedheer, B. de Groot, R. Al, M. F. Graswinckel, M. A. van den Berg, O. Kruyt, P. Smeets, H. J. van der Meiden, W. Vijvers, J. Scholten, M. van de Pol, S. Brons, W. Melissen, T. ven der Grift, R. Koch, B. Schweer, U. Samm, V. Philipps, R. A. H. Engeln, D. C. Schram, N. J. Lopes Cardozo, and A. W. Kleyn, "Construction of the plasma-wall experiment Magnum-PSI," Fusion Eng. Des. doi:10.1016/jfusengdes.2010.04.009 (to be published).
[4] G. J. van Rooij, V. P. Veremiyenko, W. J. Goedheer, B. de Groot, A. W. Kleyn, P. H. M. Smeets, T. W. Versloot, D. G. Whyte, R. Engeln, D. C. Schram, and N. J. Lopes Cardozo, Appl. Phys. Lett. **90**, 121501 (2007).
[5] M. C. M. van de Sanden, J. M. de Regt, G. M. Janssen, J. A. M. van der Mullen, D. C. Schram, and B. van der Sijde, Rev. Sci. Instrum. **63**, 3369 (1992).
[6] H. J. van der Meiden, R. S. Al, C. J. Barth, A. J. H. Donné, R. Engeln, W. J. Goedheer, B. de Groot, A. W. Kleyn, W. R. Koppers, N. J. Lopes Cardozo, M. J. van de Pol, P. R. Prins, D. C. Schram, A. E. Shumack, P. H. M. Smeets, W. A. J. Vijvers, J. Westerhout, G. M. Wright, and G. J. van Rooij, Rev. Sci. Instrum. **79**, 013505 (2008).
[7] J. Chung, R. König, J. Howard, M. Otte, and T. Klinger, Plasma Phys. Controlled Fusion **47**, 919 (2005).
[8] J. Howard, C. Michael, F. Glass, and A. Danielsson, Plasma Phys. Controlled Fusion **45**, 1143 (2003).
[9] H. R. Griem, *Spectral Line Broadening by Plasma* (Academic, New York, 1974).
[10] L. W. Veldhuizen, "Spectroscopic study of carbon chemical erosion under extreme hydrogen plasma fluxes," B.S. thesis, University Utrecht, 2007.
[11] O. Rottier, "Continuum and line emission measurements on Pilot-PSI," B.S. thesis, University of Utrecht, 2010.